Design of Integrated Bioinfiltration-Detention Urban Retrofits with Design Storm and Continuous Simulation Methods

William C. Lucas, S.M.ASCE[1]

Abstract: This article presents the elements involved in the design of a bioretention planter/trench infiltration-detention system as part of a very large-scale urban retrofit project. The prototype system was designed to intercept all of the runoff from a synthetic 5.08-mm 24-h rainfall event. Diverted flows were conveyed into bioretention planter for treatment. The bioretention systems were fingerprinted into areas comprising 0.8% of the contributory drainage areas, with an associated stone trench comprising another 3.4%. As layered systems, an approach that is capable of modeling vertical flows in addition to dynamic routing of outflows is used. The system was first modeled using HydroCAD, a design storm event modeling software. A four-compartment node system is used to model the dynamics of flow through the layers. The system was then modeled using SWMM 5.0.014 continuous simulation software. The resulting response to a design storm was computed by both of these models to compare the results of each method. The resulting SWMM model was then run on the 2005 design year rainfall distribution. Under existing conditions, over 60% of annual runoff volume exceeded the 3.50 $L \cdot s^{-1} \cdot ha^{-1}$ (0.05 cfs-ac^{-1}) threshold for initiation of combined sewer overflows (CSOs). Nearly all runoff was intercepted by the planter/trench infiltration system and even with a soil infiltration rate of only 2.54 $mm \cdot h^{-1}$, 47% was infiltrated, and less than 6% was discharged at rates that could initiate CSOs. The number of CSO exceedance pulses was reduced from 233 to 6, a reduction of 97%. The volume of flows exceeding the CSO threshold decreased by 90% in the planter/trench system.

DOI: 10.1061/(ASCE)HE.1943-5584.0000137

CE Database subject headings: Biological processes; Infiltration; Runoff; Routing; Hydrologic models; Simulation; Infiltration; Urban areas.

Author keywords: Bioretention; Infiltration; Routing; Modeling; Design storm; Continuous simulation; HydroCAD; SWMM; Bioinfiltration; Low impact development; Combined sewer overflows.

Introduction

This article presents a modeling approach to project the cumulative hydrologic responses of very extensive array of bioretention/infiltration stormwater control measures (SCMs). Bioretention systems are SCMs that typically consist of an excavated basin filled with porous media and planted with vegetation. As the storm water passes through the bioretention system, particulates are removed by filtration. Initial studies of bioretention systems documented that they offer considerable potential to retain TSS and metals, while providing encouraging results for nutrient retention (Davis et al. 2001).

There is considerable interest in such green infrastructure (GI) SCMs to reduce combined sewer overflows (CSOs). Extensive case studies are presently underway to model the projected benefits of GI in Washington, Cincinnati, Philadelphia, San Francisco, and Kansas City (LimnoTech 2009). A total of $38 million of these systems are to be constructed in the city of Philadelphia over the next year as the first phase of a Philadelphia's long-term control plan (LTCP) to reduce CSOs. In most cases, the actual design of each system will be conducted by many different consulting engineers using design storm (DS) models, which are not capable of projecting the cumulative annual response of such an extensive array of so many complex SCMs. Therefore, it is necessary to develop a continuous simulation (CS) model that can reasonably project the hydrologic response of the system as a whole. It is also necessary to ensure that the processes modeled in both the CS and DS models are treated identically. In this manner, the CS modeling can provide discharge criteria that are most appropriate for the DS modeling efforts.

While there are several models that simulate Richard's Equation dynamics in an individual layered system, they are not capable of routing outflows from the thousands of such systems needed to reduce CSOs. On the other hand, the most widely used large-scale surface flow models still use very primitive routing methods for layered bioinfiltration systems, if they are addressed at all. For instance, none of these models address unsaturated flow processes in layered systems, and I am aware of only SWMM being capable of addressing D'Arcy flow between layers; a capability only recently added. As a result, approaches that combine routing within SCM layers with dynamic wave routing of the resulting outflows have not been previously used for CSO modeling.

This article presents how runoff flows can be simultaneously

[1]Doctoral Candidate, Griffith Univ., Nathan Campus, Brisbane, Australia. E-mail: Bill.Lucas@Student.Griffith.edu.au; wlucas@integratedland.com

Note. This manuscript was submitted on December 8, 2008; approved on August 28, 2009; published online on September 1, 2009. Discussion period open until November 1, 2010; separate discussions must be submitted for individual papers. This paper is part of the ***Journal of Hydrologic Engineering***, Vol. 15, No. 6, June 1, 2010. ©ASCE, ISSN 1084-0699/2010/6-486–498/$25.00.

modeled both horizontally and vertically in both CS and DS models. In systems where extended detention is used to meet CSO discharge criteria, the dominant processes are based upon St. Venant and D'Arcy Law equations that are well understood. However, a computationally efficient approach is also needed to model infiltration responses into and from the media, and into the surrounding soils. A simple uniform infiltration rate (Φ-index) model could be used to project system infiltration responses; however, this would understate the initially rapid infiltration response of unsaturated soils. As such, projected infiltration estimates limited to saturated hydraulic conductivity can underestimate actual infiltration response in arrays of bioretention-infiltration systems. Because the contribution of initial infiltration rates is too important to entirely ignore, this paper represents a computationally efficient method to mimic (as opposed to simulate) the response of the Ψ term in the Green-Ampt infiltration equation.

Fluid transport in isotropic media comprises matric flow, characterized by hydraulic conductivity (K); and capillary suction, characterized by negative matric potential Ψ. Soil texture plays a dominant role in determining hydraulic conductivity and matric potential. Bulk density is another important determinant of infiltration properties. Higher bulk densities (compaction) are associated with lower hydraulic conductivity (Pitt 1987). Based on these properties, there is a characteristic decline in infiltration rates as a function of soil saturation. The Green-Ampt equation is derived from the Richards equation for flow through porous media (Bedient and Huber 1988, p. 45). The infiltration rate $f(t)$ at time t in the Green-Ampt equation is as follows:

$$f(t) = K_{\text{sat}}\left[1 + \frac{(\psi + h_0)\Delta\theta}{F(t)}\right] \tag{1}$$

where K_{sat}=saturated hydraulic conductivity; h_0=ponding depth on the soil surface; Ψ=capillary suction head (or negative matric potential) at the wetting front; $F(t)$ represents accumulated infiltration volume; and $\Delta\theta$=initial moisture deficit. This term is defined as the maximum water content of the soil (often assumed equal to porosity n), less the initial soil moisture content θ_i, which is usually a value intermediate between saturated and completely dry conditions. $F(t)$ represents accumulated infiltration volume; normalized by porosity, this represents saturated depth. Note that Eq. (1) includes the effect of ponding head, and under saturated conditions, it reduces to Darcy's Law.

Because it is based on relationships between specific soil properties rather than field observations, Eq. (1) is very useful inasmuch that K_{sat} and Ψ are well understood soil properties. The Pedo-Transfer Function (PTF) of Saxton and Rawls (2006) includes terms for soil texture, bulk density, salinity, and organic matter (OM). This series of 24 different equations has been used to project K_{sat}, Ψ, and available water capacity (AWC) parameters. This PTF was found to match a great proportion of field observations, thus providing considerable utility to this approach. It has been incorporated into the SPAW model (Saxton 2005). It has the advantage of addressing the effects of compaction and OM, which can substantially affect soil properties. Eq. (1) therefore has considerable utility in isotropic media where parameter measurements can be precisely obtained.

However, infiltration properties are also significantly affected by the presence of macropores. Macropores are formed by the decay of roots, the burrows of invertebrates, and shrink-swell cracks in clayey soils. Macropores are classified according to diameter, tortuousity, and connectedness. Higher values in these categories result in higher effective infiltration rates. As a result, when water is ponded at the surface, flows enter the macropores and thus can enter much more of the profile than just the wetted surface. Laminar flow G into macropores can be related to pore diameter r for a given fluid pressure p by Poiseuille's equation (Rose 2004, p. 205)

$$G = \frac{\pi r^4 \Delta p}{8\eta\Delta x} \tag{2}$$

where η=dynamic viscosity and x=depth. The second term represents the spatial gradient; assuming this gradient is the same for the same depth, Eq. (2) indicates that flow is highly dependent upon pore radius. To appreciate the importance of macropore flow, consider that macropores created by worm holes and roots are in the range of 2 mm wide, while soils without bioturbation may have pores 1/10 that diameter (Rose 2004, p. 205). Because a macropore 2 mm wide will have 10^4 times the flux of macropores 1/10 the diameter, the effect of macropores therefore exerts a substantial influence upon field infiltration rates (Novák et al. 2000). This is why infiltration rates generally remain higher in bioretention systems than in infiltration basins where vegetation is absent.

It is only recently that the literature has begun to address how media properties such as texture and OM interact with soil structure and vegetation to affect the matrix infiltration and percolation response (Sharma et al. 2006). The variable distribution of macropores is one reason why infiltration rates measured by infiltrometers vary so much over very small distances in apparently similar settings. Even in a small bioretention system, variability in infiltration rates can exceed many orders of magnitude (Nestingen et al. 2007).

On the other hand, surface clogging has the opposite effect of reducing infiltration rates, further confounding a Green-Ampt matric properties approach to infiltration, unless a layered system is involved. The median particle size of suspended solids in urban runoff is that of fine silt ($\sim$20 μm). As these fine particles settle onto the medium, they are "strained" by the bioretention medium. At the typical ratio of runoff particle size to that of a sandy medium, most of these particles are captured within short distances (Li and Davis 2008). As particles collect, infiltration rates will decline to values in the range of several centimeters per hour. Therefore, design infiltration rates will persist only if runoff is pretreated, or if the surface profile is replaced. Once the hydraulic conductivity declines enough due to particles accumulating in the media, particles then accumulate on the surface of the medium, forming a noticeable deposit (Hatt et al. 2008; Li and Davis 2008). This deposit reduces overall hydraulic conductivity to ranges from 3–11 $\text{cm}\cdot\text{h}^{-1}$ (Li and Davis 2008) to as low as 0.1 $\text{cm}\cdot\text{h}^{-1}$ (Hatt et al. 2005). Experiments by both Li and Davis (2008) and Hatt et al. (2008) show that removal of the clogging layer restores infiltration rates in heavily loaded systems.

The presence of vegetation and associated microbial processes improves infiltration properties, even where sediments accumulate (Rachman et al. 2004). Plant movement in the wind tugs at the soil surface, breaks clogging mats, and cracks through deposits (Le Coustumer et al. 2007). Ponded rainfall can then more easily penetrate clogged surface layers, increasing infiltration rates. Root turnover promotes the formation of macropores. These processes associated with vegetation are remarkably effective in restoring and/or enhancing infiltration rates. Field infiltration rates in native grass hedges can be nearly an order of magnitude higher than those found in adjacent croplands (Rachman et al. 2004; Blanco-Canqui et al. 2004a,b; Seobi et al. 2005). In bio-

retention columns, Culbertson and Hutchinson (2004) have documented that switchgrass (*Panicum virgatum*) increased infiltration rates in bare soils from 0.5 to 128 $cm \cdot h^{-1}$, an increase well over two orders of magnitude. These writers noted that the dense root system reached a 90-cm depth after a single growing season. The presence of vegetation can therefore result in infiltration rates several orders of magnitude higher than predicted by underlying soil properties (Ralston 2004). Therefore, the presence, extent, and vigor of vegetation can play as much of a role in determining soil/media response as the underlying soil texture composition.

These influences of vegetation and clogging have been documented in a field study of 21 well-established systems in Australia, with loading ratios (source to bioretention area) ranging from 5:1 to nearly 100:1. In systems averaging rapid media (20 $cm \cdot h^{-1}$ initial infiltration rates), infiltration rates declined toward an average of 10 $cm \cdot h^{-1}$, presumably due to clogging, while in slow media (1 $cm \cdot h^{-1}$ initial rates), rates improved to 2 $cm \cdot h^{-1}$, presumably due to the development of macropores (Le Coustumer et al. 2007). While allocating a specific mean value for variables such as K_{sat} and Ψ will only rarely represent the cumulative response of the system, this is the best that can expected in the engineering design environment.

In a loamy sand bioretention media, initial infiltration rates decline in the manner characteristic of the Green-Ampt response. However, outflows are much more rapid than would be expected from matric flow properties, suggesting extensive macropore flows (Lucas and Greenway 2007). Hallam and Carpenter (2008) reported outflows within 15 min after inflows in media 75 cm deep with a K_{sat} of 45 $cm \cdot h^{-1}$ and a porosity of 50%. Given the very high water holding capacity of the compost media, outflow occurred more rapidly than would be expected based upon the advance of a wetting front. In a 120-cm-deep loamy sand bioretention cell with a laboratory permeability rate of 1.1 $cm \cdot h^{-1}$, Hunt et al. (2008) reported outflow an hour after rainfall began, suggesting an effective infiltration rate well over an order of magnitude faster than matric flow. Applying a 16:1 loading ratio to 16-mm rainfall, the 26-cm accumulated depth is little more than one-half the porosity available. In addition, while these outflow responses suggest macropore flow in media with even high infiltration rates, the drainage response can also be quite swift. Hallam and Carpenter (2008) reported that outflow persisted for less than an hour after inflow ceased, while Lucas and Greenway (2007) reported a draining time of 2.5 h. On the other hand, outflows persisted for over 12 h after rainfall ended in the deeper media of Hunt et al. (2008). More research is needed to correlate the effects of vegetation and media composition on drainage properties.

To summarize, studies of flow through isotropic porous media are well represented in the extensive literature on liquid transport, but the effect of vegetation upon infiltration has only recently been addressed, and even then, largely from an observational basis (Blanco-Canqui et al. 2004a,b). Even though the effect of vegetation can increase infiltration rates by an order of magnitude, there is virtually no published literature proposing a process-based model that addresses the effect of vegetation upon infiltration. The preceding suggests that classical infiltration approaches based on flow through isotropic media are only a point of departure for examining bioretention systems. While the Green-Ampt formulation may be accurate under certain conditions, it is a fallacy to assume that it is the most representative, unless supported by parameters that reflect vegetative influences. Notwithstanding this limitation, it does afford the ability to account for head, and the resulting changes in infiltration rates as determined by Darcy's Law. These aspects of the Green-Ampt formulation make it attractive for modeling.

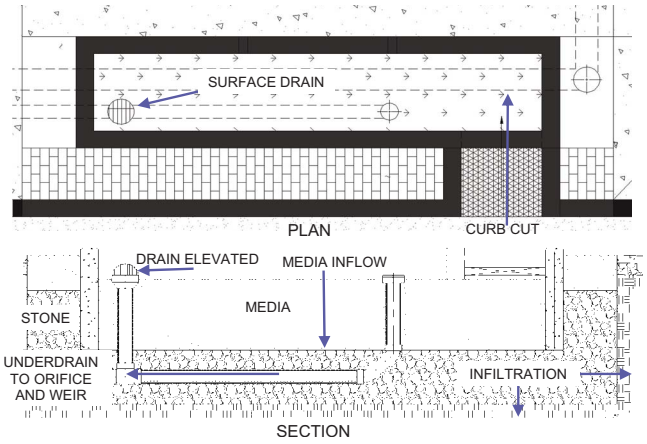

Fig. 1. Layout and elevation view of typical planter system (courtesy of CDM and PWD)

Methods

System Design

Fig. 1 displays the plan and elevation view of the bioinfiltration systems, showing the various different compartments through which runoff flows. Inflow from the street initially flows onto the bioretention media, from which it either passes through the media, or enters an overflow inlet. This inlet is situated above the surface of the media in order to promote preferential flow through the media. Media and bypass flows then enter a subsurface infiltration trench, from which accumulated runoff either infiltrates into the soil, or is discharged through the underdrain.

A key aspect of this arrangement is the fact that flows under saturated conditions are driven by hydraulic gradients, so backwater created by any of these nodes will control system response. In this case, the underdrain is controlled by an orifice to maximize detention time and reduce flows as much as possible to meet CSO reduction thresholds. Unsaturated flows from the media are minimal given detention times of several days, so media drainage responses can be ignored. The major variables that remain are that of infiltration into media and into the soil. A quasi-Green-Ampt approach based upon orifice flow is used to mimic the initial infiltration response into the media and into the soil. This simplification is justified given the complexity of infiltration responses discussed above which cannot be modeled accurately even with Green-Ampt equation.

The systems were first modeled with HydroCAD8.5 DS software, which is based on the curve number (CN) method. The systems were then modeled using SWMM 5.0.14 CS software, which uses kinematic wave routing for runoff and dynamic wave routing of conduits and storage nodes. In this manner, a greater appreciation of the dynamics of the system can be observed, and appropriate discharge criteria for DS designs can be obtained from the results of the CS analysis. This considerably enhances the potential that the typical DS models used by most of the design and regulatory community will obtain suitable designs that would otherwise require considerably more effort involved in CS

modeling. This is particularly important when designing these systems to meet the 3.50 $L \cdot s^{-1} \cdot ha^{-1}$ (0.05 cfs-ac^{-1}) threshold for CSOs to occur.

Two bioretention planters linked by a stone trench were designed to provide storage of at least 25.4 mm (1 in.) of runoff from the surrounding impervious areas. This system is sized to treat the runoff contributing to a typical storm inlet. It is intended to not only intercept runoff from frequent events, but also to infiltrate as much of it as possible. The balance that does not infiltrate is released through a small orifice at the end of the underdrain to reduce flows below the 3.50 $L \cdot s^{-1} \cdot ha^{-1}$ CSO threshold. Each planter comprises a 5.08 m long by 91 cm wide (16.67 ft by 3.0 ft) cast in place concrete cell. The planter media is placed at a depth of 81 cm (32 in.), with the top being 41 cm (16 in.) below the lip of the planter. This results in the media being 10 cm (4 in.) below street elevation. Runoff from the street is intercepted by a 91-cm-wide curb cut placed 5 cm above the media to prevent backwash of mulch from the planter. The planters are placed upon a stone bed of AASHTO no. 57 stone with a compacted void percentage of at least 40%. This bed is 61 cm (2 ft) deep, and extends 61 cm beyond the ends and 25 cm wide on the sides the planter. It is extended up to the sidewalk section. Fig. 1 displays the plan view and sections of the planters.

Runoff collected in the planters initially passes through the planting media, and once ponding depths exceed 5 cm, also pass through an 46-cm circular inlet and then into an 20 cm (8 in.) distribution manifold into the underlying stone. Given this internal bypass arrangement, these systems are capable of intercepting runoff very effectively in even large events, while treating the smaller events as flow through the media for better treatment performance. Between the planters, there is a 23.9 m long by 1.5 m wide (78.5 ft by 5 ft) infiltration trench 152 cm deep, with its bottom set this distance below street elevation. This trench is also filled with no. 57 stone. Darcy flow computations showed that flow through the stone would not be able to transfer incoming runoff rapidly enough to intercept flows. Therefore, to better utilize the capacity of the trench, the inflow distribution manifold is also extended into the trench by 6.1 m (20 ft).

Runoff accumulated in the stone system is collected by a perforated underdrain that discharges into a control structure comprising a 13 mm (0.52 in.) circular orifice at the underdrain invert, and a 61 cm (24 in.) wide overflow compound v-notch weir 122 cm (48 in.) higher. Because the underdrain is surrounded by drainage geotextile to prevent entry of fines in the discharged flows, this design should eliminate the potential for a clogged orifice. Although infiltration tests at the locations of the planters indicated negligible infiltration, the extent of the area exposed by the trench is likely to encounter areas of some infiltration. As a result, the nominal infiltration rate of the soil surrounding the trench was projected at 2.54 $mm \cdot h^{-1}$ (0.10 $in. \cdot h^{-1}$) per hour. This rate is applied to the sidewalk side and bottom of the trench and surrounds. The street side is isolated by an impermeable membrane to prevent excess moisture in the subgrade from inducing soil instability. Table 1 presents a summary of the source and treatment areas.

The mineral component of the media used in the planters is comprised of 85–90% US Golf Association (USGA) turf sand by weight, which has a high uniformity coefficient and an effective pore size (d_{10}) of ±0.10 mm. The balance of the mineral component comprises loam topsoil with no more than 40% clay. The total percentage of clay in the media does not exceed 5%. In addition to these mineral components, 15% by volume of coir peat is blended into the media. This provides additional water holding capacity, soil tilth, and improves infiltration properties. The media is placed on a woven geotextile with an apparent opening area no less than 30%. The media is placed in lightly compacted lifts to the design elevation, after which it is soaked and raked level, and then soaked again to settle closer to final grades. After raking, the media is then resoaked and leveled before the final lift of media is placed. A 10% compost by volume is added to the last lift to improve plant germination and water holding capacity. The projected void percentage of the media of 30% represents the difference in water storage between saturation and field capacity. Depending upon settlement, the saturated hydraulic conductivity is projected between 20 and 50 $cm \cdot h^{-1}$ (8–20 $in. \cdot h^{-1}$). To account for potential clogging at the surface, the design infiltration rate of the media is projected at 10 $cm \cdot h^{-1}$ (4 $in. \cdot h^{-1}$). Table 1 sets forth the source areas, treatment areas, and provided storage of each SCM.

Table 1. Source Areas and Design Parameters of the SCM Systems

SCM label	Source area (m^2)	SCM area (m^2)	SCM depth (m^2)	Void (%)	SCM volume (m^3)	SCM volume (cm)
Planter no. 1	479.8	4.65	1.52	30–40	2.73	0.57
Planter no. 2	556.0	4.65	1.52	30–40	2.73	0.49
Trench		39.44	1.52	40	24.04	2.32
Combined	1,035.8	48.73	1.52	30–40	29.51	2.85

Design Storm Events

Because this evaluation is intended to examine SCM performance as opposed to meeting standard flood criteria, the NRCS type II rainfall distribution DS typically used for flooding analysis in Philadelphia is inappropriate. A synthetic storm designed to represent the addition of a series of individual DSs has very little basis in observed storm events. Instead, the more realistic "Sample D" DS rainfall distribution was used for evaluating the SCMs. Fig. 2 displays the difference between these events in terms of peak rates. The type II DS is very abrupt compared to the Sample D distribution. This is particularly important in terms of evaluating system capture, as an artificially high peak rate will understate interception. Because there is more rainfall in the Sample D design event during the rising and recession limbs,

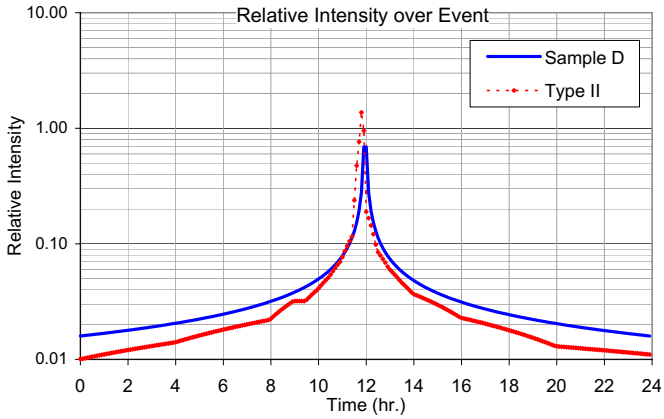

Fig. 2. Comparison of type II (higher peak) to Sample D (lower peak) DSs

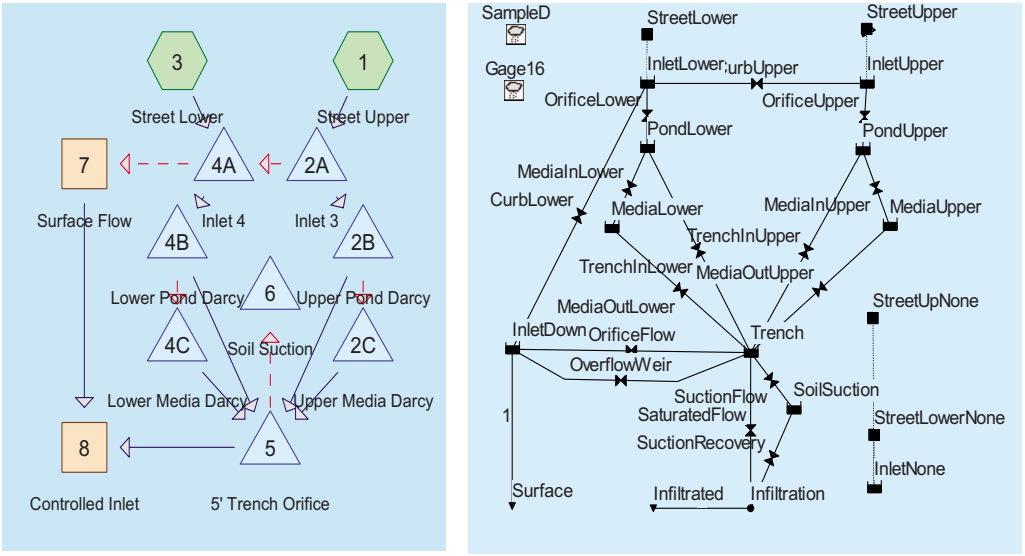

Fig. 3. Model routing diagrams: (a) HydroCAD8.0; (b) SWMM 5.0.14

bioretention infiltration rates can better capture flows. Figs. 7 and 8 present hyetographs of the largest four events, in which all but one are much less peaky than the type II event.

The hydrographs presented in the analysis evaluate the Sample D 24-h rainfall distribution for the 50.8 mm (2.00 in.) event. The latter represents the 24-h event with an average recurrence interval of approximately nine months. Events up to this size cover most of the events of interest in evaluating annual SCM performance. To compare design results between HydroCAD and SWMM, it is necessary to ensure that flows into the SCM systems are identical. Because runoff from these DSs were generated by different modeling algorithms (kinematic wave versus hydrograph convolution), it was necessary to adjust the subcatchment characteristics to generate runoff responses as identical as possible. In HydroCAD, the typical CN for impervious areas was adjusted upward to 100, thus eliminating the effect of initial abstraction. The depression storage factor in SWMM was likewise adjusted to none. The time of concentration in HydroCAD was set at 28 min to give the same peak timing as SWMM, using a catchment width of 100 ft. Comparison of the resulting runoff hydrographs showed virtually identical shapes and total volumes. Because these conditions exclude initial abstraction, the "effective" source area shown in Table 1 is increased by almost 13% in the 50.8-mm event.

Routing Setup-Design Storms

To represent the system, it is necessary to disaggregate the various components so they can be modeled discretely. As shown in the routing diagram in Fig. 3, this is accomplished through modeling the contributing subareas individually (1 and 3). Each bioretention/surround system is then subdivided into three nodes: an inlet node (2A and 4A), a planter pond node (2B and 4B), and a media node (2C and 4C). The planter surround stone and trench stone are combined into one trench node (5), which is filled by flows through the media and bypass flows from the surface pond of each planter. These are shown as primary flow in solid blue arrows. The corresponding SWMM5 routing diagram is presented to facilitate comparison.

The inlet orifices are modeled explicitly to ensure that they do not constrain flows. Overflows down the street are shown as secondary flows in dashed red arrows. These flows represent bypass flow to a surface node (7) that is not intercepted by the planters. Intercepted flows pass from the inlet into the planter pond node set at an elevation 10 cm below the street. This small hydraulic gradient drives the entire system. No separate outlet to the street is provided, because flows will not enter the system once the ponding elevation inside the planter matches the flow elevation in the street, which is set as a triangular weir conforming to the street cross section geometry.

To route flows into the media, a constant rate infiltration approach is often overly conservative because it does not represent the typical Green-Ampt response in which initial rates are several multiples of final rates. Nor does it respond to Darcy's Law, which increases rates of flow as runoff ponds on the surface of the media and, conversely, decreases flows when the media is saturated and outflow is restricted. Thus, this method can both substantially underestimate and/or overestimate infiltration rates into the media. For these reasons, the uniform rate approach is not used in this paper.

To address the initially high rates when the media is still wetting it is possible to use SWMM5's capability to model Green-Ampt responses explicitly as a receiving "subcatchment." However, SWMM5.0.14 provides no way to account for flows into such a subcatchment if it is restricted by hydraulic gradient from underlying compartments that would eliminate effective head. Therefore, because a fixed rate approach neither represents realistic infiltration dynamics, while a Darcy's Law response is not possible in a SWMM5 subcatchment, an alternative approach is needed to reproduce such vertical flow dynamics in both DS and CS environments.

One possibility for an improved approach is to model the flows into the media as if they were routed through an orifice. This approach obviously does not replicate the complexity of unsaturated flow dynamics into and through a complex media/soil system of several layers. Furthermore, orifices increase flow at the half-power of head, while Darcy's Law through media of a uniform length bears a linear relationship to head. Therefore, orifice responses will be at best an approximation. However, because ponding depths that increase flows into media are so shallow, allocating an orifice several inches below the surface is an effec-

tive method to mimic initial inflows into the media. Flows are initially higher than stabilized rates until head in the media rises, thus mimicking Green-Ampt response, while the orifice will then respond to the hydraulic gradient when the media is saturated.

For flow through the media, HydroCAD offers a flow routing option that permits flows through elevation-dependent rating curves that reflect the difference in head between nodes. With this option, the rating curve flow declines once there is less effective head. This often occurs when outflow is controlled by infiltration into the surrounding soils. In this manner, the outflows can respond according to the limiting condition. To do so, the hydraulic grade line must be carried upward from the surrounding soils through the media into the pond, and even back out the inlet in extreme events. As a result, there can be minimal flow into or through the media once the surrounding stone is filled up and outflows are restricted by its discharge response. This method can provide quite a reasonable representation of flows into and through the media when it is saturated. To dampen oscillations at such shallow depths given the minimum time step of 36 s in HydroCAD, the systems were multiplied by a factor of 10. The media nodes were modified to include a small "dummy" area that extends upward into the overlying pond node. Given the small depths involved, this introduces only a slight bias in the results.

It is only very recently that the SWMM version 5.0.014 has offered the same capability to use outlets based on rating curves sensitive to hydraulic grade. This is shown as the tabular/head or functional/head options for the outlets. So, it is now possible to model Darcy's Law accurately to project flows through the media as a function of effective head in both the CS and DS environment. Because media depth is fixed, it is a simple computation to project flow rates according to the simplified case of Eq. (1), using a coefficient based on infiltration divided by media depth, applied to head at a power of one.

Because the planter area of the systems is only 0.8% of the effective source area, even relatively small events will exceed the infiltration rates into the media, resulting in surface ponding. Once the surface ponding exceeds the bypass inlet grate set 5 cm higher, the resulting flows are also routed through the bypass inlet into the stone surround and trench system as primary flows. Accumulated runoff into the combined surround and trench stone system is collected by a perforated underdrain that discharges into a control structure comprised of an orifice and the compound v-notch overflow weir. The latter is routed as secondary flow to highlight its contribution to total flows. Because infiltration rates are so low, this system is designed to release accumulated runoff into the collection system at rates less than $3.50\ \mathrm{L\cdot s^{-1}\cdot ha^{-1}}$ ($0.05\ \mathrm{cfs\text{-}ac^{-1}}$) through the orifice, routed as primary flows. These flows enter existing inlet (8).

Flows passing through the trench node infiltrate into the surrounding soil at a K_{sat} projected to be $2.54\ \mathrm{mm\cdot h^{-1}}$. Outflows from this node are allocated by rating curves calculated according to the corresponding wetted area and K_{sat}. However, in addition to saturated flows, it is necessary to mimic the capillary suction response of the surrounding soil. This is accomplished by creating a dummy node (6) 413 cm (13.55 ft) below the bottom of the trench. The dummy node area is sized according to the projected capillary suction depth multiplied by the bottom surface area to obtain the suction volume, which is then divided by this depth. Flows enter the node through an orifice at the bottom which is sized to represent the initial peak rate. This rate is based on the ratio of capillary suction to K_{sat}, divided by a factor of 5 to account for the great disparity between these values in poorly infiltrating soils with low K_{sat} and high capillary suction. In this case,

Media Void%	30%	Stone Void%	40%
MEDIA DATA			10.16 Ksat (cm/hr)
Length 50.81		Width 0.91	
Elevation (m)	Area (sq.m)	Head (rel.)	Volume	Pore Vol.	Q (lps)
4.74	46.5	0.125	0.0	0.0	0.16
5.01	46.5	0.250	12.6	3.8	0.33
5.28	46.5	0.500	25.2	7.6	0.66
5.55	46.5	1.000	37.8	11.3	1.31
SWMM	13.9	0.271	Interval		
INTO MEDIA		No.	1	Diameter	5.243
Or.Area (sq.cm.)	21.5862	Head (cm.)	5.18	Design Q (lps)	1.3052
FROM MEDIA		Length (cm)	81.38	Darcy (lps/m)	1.6112
INFLOW UNDERDRAIN DATA				Or.	0.7432
Dia (cm.)	30.48	Area/m	0.958	No. per m	39
elev	Length	No.	Or. Area	Or. Rate	Q (lps)
4.21	25.4	1000	743.37	223.27	4.08
TRENCH DATA				0.254	Ksat
Underdrain		Length	403.86	Width	1.52
Surround/Trench		Length	320.04	Width	1.52
Elevation	Bottom	Side Area	Sides	Q (lps)	Ksat
4.13	615.5	0.0	0.0000	0.4343	0.3961
4.74	615.5	247.1	0.1744	0.6086	0.5704
SWMM	246.2	Pore Vol.	150.1		
4.74	425.8	0.0	0.0000	0.6086	0.5704
5.55	425.8	261.7	0.1846	0.7933	0.7551
SWMM	170.3	Pore Vol.	138.6		
SUCTION DESIGN					
Suction (cm)	17.8	Diameter (cm)	3.810	Peak Q (lps)	6.080
Suction Ratio	14.0	Or.Area (sq.cm)	11.401	Design Q (lps)	5.996
Recovery (hr)	237.2	Depth (m)	4.13	Rise Vol.(cu.m)	32.83
Recovery (lps)	0.0382	Area (sq.m)	7.9	Node Vol.(cu.m)	32.62
OUTFLOW UNDERDRAIN DATA				3810 (cm/hr)	
elev	Area	Flow	Perfs	Rate (lps)	Q (cfs)
4.21	48.7	514.92	743.37	106.20	106.20
Diameter	4.05	Orifice	12.9069	Design Q	4.082

Fig. 4. Storage, outlet, and flow rating curves for Darcy's Law/orifice controlled planter/trench systems

this ratio of 70 is divided by 5 to give a suction ratio of 14, or an initial rate of $3.6\ \mathrm{cm\cdot h^{-1}}$ into dry soils. Given this configuration, flow rates into this node are initially rapid due to the high head across the orifice, and then decline as the soil node fills up (saturates) and the effective head differential declines. Fig. 4 presents a summary spreadsheet showing the various input parameters of these nodes and links.

To simulate recovery of suction, flows leave this soil node at a constant outflow based the SWMM recovery equations (James et al. 2008, p. 468)

$$T = \frac{\sqrt{K_{sat}}}{75} \tag{3}$$

where T=time in hours to restore dry conditions form complete saturation. The suction volume is divided by this rate to obtain the recovery rate. This rate is subtracted from the rating curve for saturated conductivity to avoid double counting. In this manner, there will be minimal suction flow for events that occur when the suction node is full (wet), while events that occur when it has drained will have a greater suction response. Essentially, this suction node operates as a sponge with the capacity representing the

suction head volume, designed in a manner that accelerates the same infiltrated volume that would be determined by a constant K_{sat}.

While these artifices obviously oversimplify the processes involved, the system response throughout an event is quite similar to that expected from a more physically process-based model, while requiring considerably fewer computational resources. Given that errors in parameter estimation, particularly K_{sat}, are just as important in the Green-Ampt approach; an explicit process-based approach may not be that much more valid. The orifice/Darcy's Law method is a more efficient computational method that can run more scenarios in a given time; preferable to modeling fewer scenarios with perhaps greater precision, but not necessarily greater accuracy. The distinction is important when modeling large arrays of these systems for a city the size of Philadelphia.

Routing Setup-Continuous Simulation

The same stage area-outflow responses shown in Fig. 4 were entered into SWMM 5.0.014. Unlike HydroCAD, where both storage and outflow parameters are entered for each storage node, SWMM5 lists each orifice weir and outlet as a separate links from the associated storages node. These corresponding additional links are also displayed in the routing diagram shown in Fig. 3. The links between the pond media and trench nodes are self-explanatory. Flows from the trench pass through the orifice representing the suction flow component of infiltration (SuctionFlow) into the matric suction node (SoilSuction), while saturated flows (SaturatedFlow) passes directly into the surrounding soil (Infiltration), along with recovery flows from the SoilSuction node. The SaturatedFlow into the surrounding soil was set at the wetted area rating curves for saturated hydraulic conductivity, as reduced by the flow rate applied to the SuctionRecovery node. This flow has no backwater, so standard rating curves are used. Because SWMM cannot discharge through an outlet unless its storage range includes the outlet elevation, a narrow dummy cylinder was extended down from the trench to the SuctionFlow orifice elevation. As a result, the trench node very rapidly fills to the design elevation, immediately increasing head, while the SoilSuction node elevations rise less rapidly. The same orifice and overflow weir arrangement used in HydroCAD was used to discharge surface flows. In all hydraulic respects, the SWMM input was identical to the HydroCAD input files for the comparison study. To facilitate assessment, the comparison study used less suction volume (6.25 cm) and more rapid recovery rate ($0.145\ L \cdot s^{-1}$) than that shown in Fig. 4.

In addition to the same Sample D rainfall distribution events used for the HydroCAD computations, SWMM used a CS time series rainfall file to project annual responses. This distribution is the 2005 "synthetic year" distribution developed by Camp Dresser and McKee (CDM) based on 26 years of rainfall records. This design year was selected as being hydrologically representative of annual rainfall distributions, subject to including several larger events to address flooding design. An uncontrolled system without the SCMs (InletNone) was established for comparison purposes. he CS model was then used to compare flow distributions of the uncontrolled system to the planter-trench low impact development (LID) system in terms of reducing overall runoff, and in particular, reducing CSOs. A threshold of $3.50\ L \cdot s^{-1} \cdot ha^{-1}$ ($0.50\ cfs\text{-}ac^{-1}$) was set as the runoff rate at which CSOs are likely to occur.

In the CS modeling, the suction node volume was increased to 17.8 cm while the recovery rate was reduced to $0.038\ L \cdot s^{-1}$ per Eq. (3), adjustments which considerably delayed the recovery of suction. As a result, the suction node would have negative flow by draining back out of the trench underdrain, which is not what would occur in reality. This is why different values were used for the CS/DS comparison. To resolve this, a flap gate was placed on the inflow link to prevent backflow, which prevented this artifact from generating unrealistic system dynamics.

Results and Discussion

This disaggregated routing results in unexpected behavior during events as the various compartments fill and empty at different rates. Fig. 5 presents the resulting orifice/Darcy Law responses of the HydroCAD compared to SWMM in the 5.08 cm (2.00 in.) Sample D event. Table 2 presents the resulting volumes for these methods. In all parameter responses, note how the SWMM and HydroCAD results are virtually identical in terms of peak flows, node elevations, and the timing of responses. The volumes diverted to each node were also very similar for both orifice-based approaches. As such, the SWMM model replicates HydroCAD results during flow events with a high degree of correspondence. This supports the concept of relating the results of DS models to CS models, and vice versa. Even though the recovery dynamics in HydroCAD differ from SWMM, as a DS model, the dynamics of suction recovery modeling are not applicable in any event.

Inspection of the media response in Figs. 5(a–c) shows several features. The initial orifice controlled inflow rates into the media shown in Fig. 5(a) are as high as inflow rates into the pond until hour 6, when the media becomes saturated and inflows are then controlled by the system based on Darcy's Law. This response effectively mimics the suction response expected in initially dry media. Note how the Darcy's Law method applied to media outflow delays both the initial onset and final recession limb of flows from the media. The initial outflow lags inflow by an hour, occurring when the media is only partially saturated. The media recession limb persists for 12 h after inflow ceases, as the trench itself drains. There is a pronounced secondary peak in both the media inflow and outflow response. This is due to flows entering the media abruptly declining once the surrounding stone is temporarily filled up, thus eliminating effective head. This corresponds to the trench inflow peak shown in Fig. 5(d). Once peak inflow passes, flows then increase as the stone drains, providing more hydraulic gradient.

Figs. 5(e and f) display the resultant trench and surrounding soil responses. Recall that the surrounding soil node is set at a depth well below the trench to promote rapid initial flow due to high relative head. This is shown in Fig. 5(e), where it is apparent that the corresponding narrow column in the trench rapidly fills up, resulting in a substantial head relative to the SoilSuction Node from hours 0 to 6. This head results in the peak in trench outflows from hours 0 to 6 shown in Fig. 5(f). Constrained by the inflow rate, the rising limb peaks at hour 3, and then declines by hour 6 as the SoilSuction node fills up to the elevation of the trench, as shown in Fig. 5(e). A smaller secondary peak occurs at hour 12 when inflow intensities are greatest, so more surface area is exposed to wetting. This is also a result of a difference in elevations between these nodes. When the surrounding soil elevations peak at hour 14, the infiltration rate from the trench declines to a rate that is slightly higher than projected by the constant rate applied to wetted area. The difference between SWWM and HydroCAD

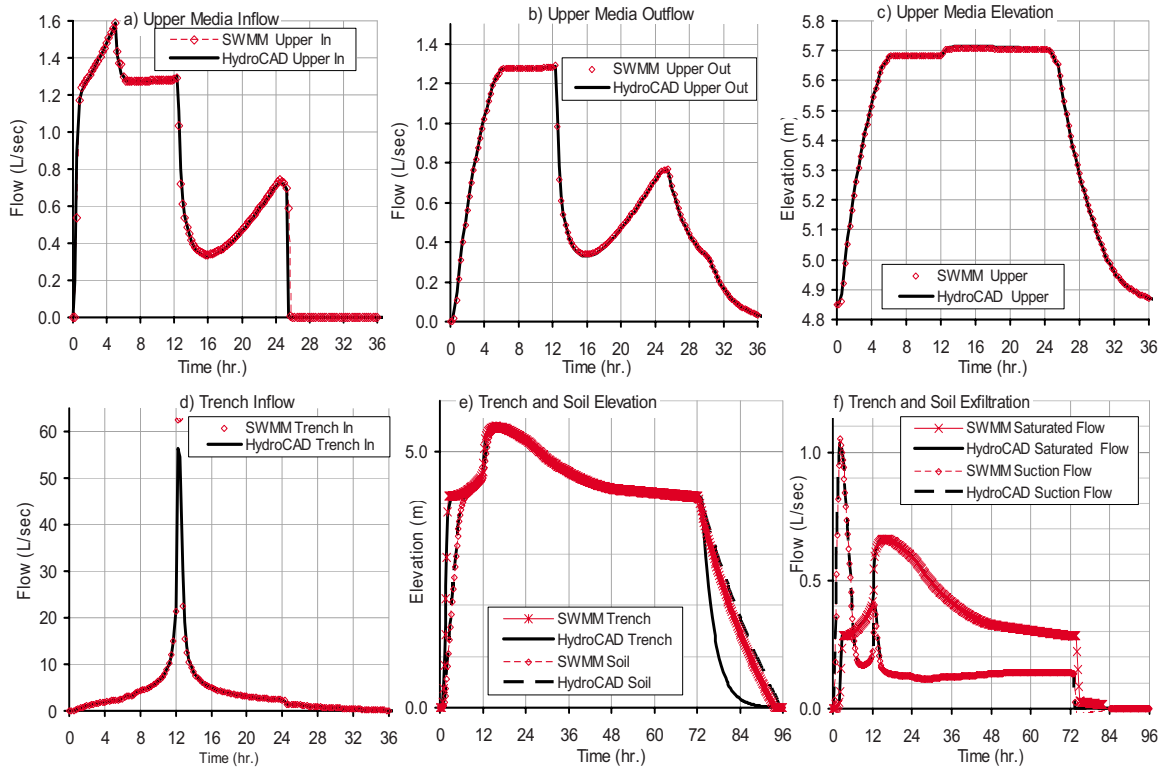

Fig. 5. Comparison of orifice controlled systems during 2.00-in. Sample D event, HydroCAD, and SWWM models: (a) upper media inflow; (b) upper media outflow; (c) upper media depth; (d) trench inflow; (e) depth in trench and surrounding soil; and (f) flow from trench into surrounding soil, saturated and suction flows (suction reduced and recovery accelerated)

during drainage in Fig. 6(e) is due to orifice flow not reversing in HydroCAD as it does in SWMM.

This response "front loads" the infiltration response, as would be expected from a Green-Ampt response. While the decay from initial rates may be an approximation of matric processes, the approach using a suction node seems to provide reasonable results for CS modeling. Fig. 6 displays the response using the parameters set forth in Fig. 4 for the 2005 design year. The long storage time within the system and slow recovery period results in partially to fully saturated conditions through most of the year, as shown where the node head is elevated at or above the bottom of the trench at 4.13 m. There are only a few occasions when the system is completely dry. Note how the corresponding suction responses show much greater amplitude during these periods, while the suction response is completely attenuated when the system is saturated. Such responses would be expected from a system that retains runoff long after rainfall ceases.

Table 2. Inflow and Outflow Volumes (m^3), 5.08 cm (2.00 in.) Sample D Event

SCM label	Pond upper	Pond lower	Upper media	Lower media	Trench
HydroCAD, orifice flow, and Darcy's Law					
Inflow	282.5	243.7	81.0	71.8	526.2
Primary	201.5	171.9	81.0	71.8	373.9
Secondary	81.0	71.8			152.3
SWMM, orifice flow, and Darcy's Law					
Inflow	282.5	243.7	81.1	71.9	526.7
Primary	201.8	172.3	81.1	71.9	373.6
Secondary	81.1	71.9			152.7

Fig. 7 displays the SWMM responses to a variety of flow hydrographs during the 2005 design year. The April 2 response occurs when the suction node is only partially drained below the trench. During the initial and final rainfall pulses, the proportion of suction is relatively high as the trench fills up above the suction node. The intervening transient suction responses at each rainfall pulse are relatively small. Note how the suction response diminishes within an hour, as would be expected. Compared to saturated flows, the overall contribution of suction is relatively minor. In contrast, the intense event of August 15 occurs when the system is drier, so the differential head is greater. In this case, the suction rate is many times higher than the saturated response. Due to the fact that the trench is completely filled during this short event, the increase in wetted areas results in a suction response that persists for several hours. A mixed response occurs during the October 8 event when the system is initially dry, followed by much smaller responses until a final suction response that occurs as the sidewalls become fully wetted before the trench overflows. As the largest event of the year, total precipitation depth was 9.83 cm.

To examine the potential responses at a higher infiltration rate, saturated hydraulic conductivity was increased to 1.27 $cm \cdot h^{-1}$ (0.50 $in. \cdot h^{-1}$), while suction head was reduced to 6.4 cm (2.5 in.). As shown in Fig. 8, the increased infiltration rate had substantial effect upon the three largest exceedance events in the 2005 design year. While there were CSO exceedances in all three events, the exceedance volume and peak flows were substantially reduced, and the peaks were lagged by the increased infiltrated volume. These reduced flows are correlated with the lower trench eleva-

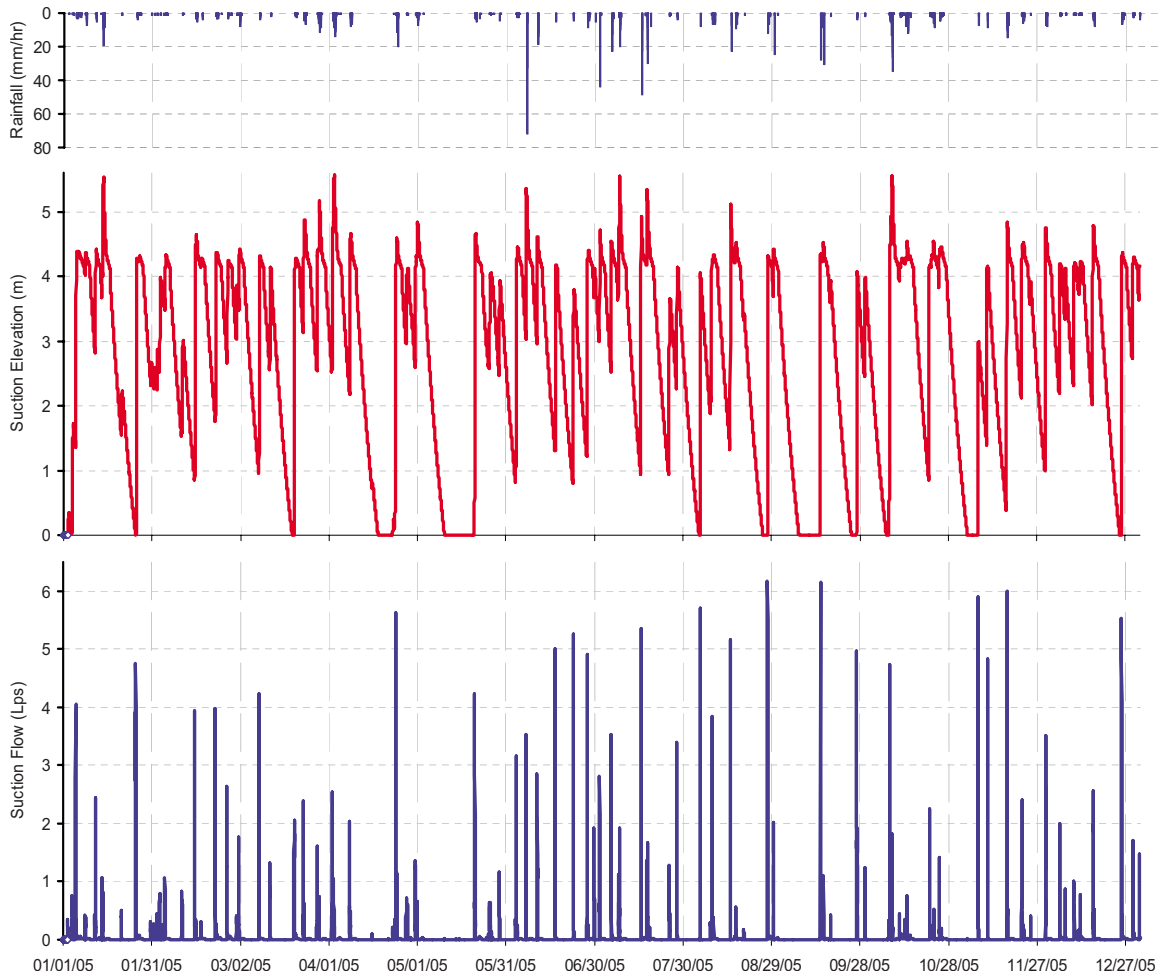

Fig. 6. Annual suction response, 2005 design year. Top row displays rainfall, middle row displays suction node elevation. Bottom row displays trench outflow into surrounding soil via suction flow.

tion resulting from the higher saturated conductivity. A scenario run with no suction at this higher K_{sat} found virtually no difference in the hydrographs. This is apparently due to the fact that the relative volume of suction was not only reduced compared to the low conductivity scenario; it was also rapidly transmitted through the suction node by its much faster recovery rates.

Along with the preceding three scenarios, another scenario run with no suction applied to the 2.54 $mm \cdot h^{-1}$ K_{sat} case was conducted to see how important the suction component would be in tight soils under the high loading of the systems. Table 3 presents the results of the various scenario comparisons. Even allocated with a very low K_{sat} of 2.54 $mm \cdot h^{-1}$, runoff volume from the SCM systems was reduced from 1,175 to 680 m^3. This represents a discharge reduction of 42%. Though not designed for large events, the peak flows were also reduced by 56%. While these are substantial reductions in annual runoff, the number of CSO exceedances declined even more, from 233 to only 6 events, a decrease of 97%. Of these events, only the three shown in Fig. 8 had substantial flows. As a result, the volume of exceedances was reduced from 635 to 72 m^3, a reduction of 90%, and the duration of exceedances declined by 90%.

As would be expected, the scenario without suction routing performed worse than the scenario with the suction. Table 3 displays that the proportion of infiltrated flows routed by this pathway was 121 m^3, or 24% of the infiltrated volume. Note that this value is almost three times the 8.9% difference in infiltration volumes, suggesting that the suction routing approach only moderately enhances infiltration performance estimates in tight soils. Notwithstanding, such a difference is still important when applied to large arrays of these systems. Note that this response reflects the long detention time where a suction response would be absent due to saturated conditions. In less intensely loaded systems, the relative proportion would be higher.

When K_{sat} was increased to 12.7 $mm \cdot h^{-1}$, the percentage infiltrated increased to 77%, with 912 m^3 infiltrated. The number of exceedances was reduced by 98% to only 4. The volume of exceedances was reduced to 34 m^3, a reduction of 95%, and the duration of exceedances also declined by 95%. Note that these results were obtained at infiltration rates that are still quite low. The percentage of flows routed by the suction approach was only 15%, while the difference in volumes was less than 1%. This highlights how the suction approach is most applicable to tighter soils.

Table 3 also presents the extent of flows that are treated by the media. In all three scenarios, the percent of total runoff treated by flow through the media is at least 44%, a remarkable proportion for a SCM with a surface area of only 0.8% of the source area. While the remaining runoff volume may not be treated by the media, it represents not only the less polluted flows that occur after the first flush; such flows are also filtered both by passing through the planter vegetation and then through the stone. These results emphasize just how effective a bio/infiltration SCM sys-

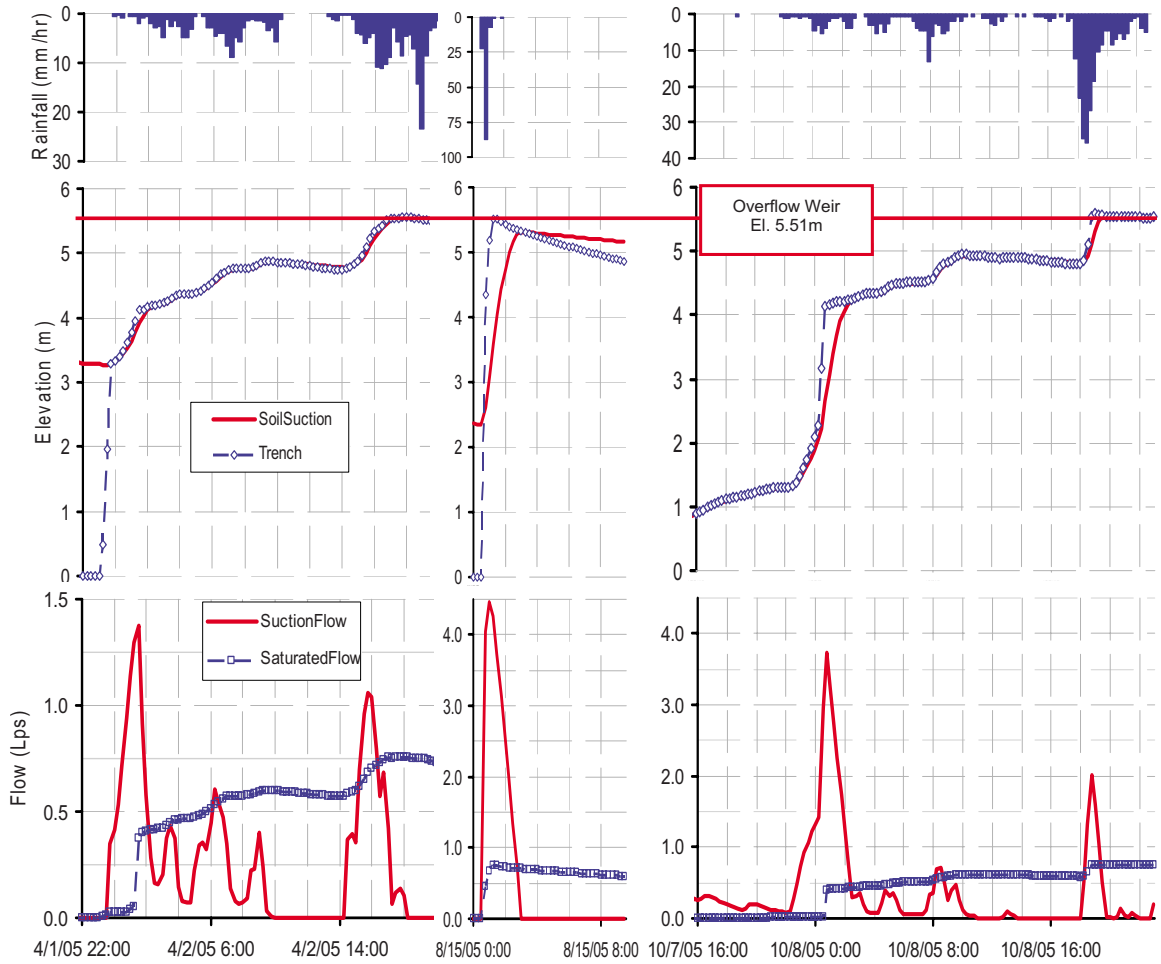

Fig. 7. Infiltration flow rates and node depths: (a) April 2, 2005; (b) August 15, 2005; and (c) October 8, 2005. Top row displays rainfall. Middle row displays trench and suction node elevations. Bottom row displays trench outflow into surrounding soil via suction and saturated flow. Note differing scales for rainfall and flow.

tem can be, even when constrained by very low infiltration rates into the surrounding soil. This is due to the extensive surface area and extended detention time in the system.

Fig. 9 graphically displays how the resulting annual flows are distributed. This graph uses the typical percent exceedance display, as shown with the open symbols on the upper abscissa. In the exceedance distribution, flows are apportioned across the entire range of percentages, because they are normalized in terms of total flow. However, flows are not only altered in terms of their distribution, they are also reduced in terms of total magnitude. To better display the comparison of the LID scenario to the uncontrolled scenario, the data are plotted on the bottom abscissa in 15-min flow intervals. While this method shows similar trends in flow distributions, its extents are different. Because cumulative flows are not normalized against themselves, they represent a better comparison between treatments with different flow volumes.

Without SCMs, flows exceed the CSO threshold over 30% of the time. With the SCM system at the K_{sat} of 2.54 mm·h^{-1}, the percent of time that flows exceed the CSO threshold then declines to 1% of total runoff duration. However, because total flows are different between these scenarios, it is difficult to compare what this difference in percentage means. The interval flow plots show a more comprehensive picture. In the no LID scenario, there are nearly 800 flow intervals over the CSO threshold, with the remaining 1,600 or so intervals below the threshold. In contrast, there are only 40 intervals over the threshold in the LID scenario, while there are some 4,400 flow intervals are below the threshold. So even though there are many more flow intervals in the LID scenario, their flow rates are relatively low. Essentially, these low surface discharge flows make up for the low infiltration rates. This type of observation is not readily apparent from the percentage graphs. Furthermore, it can be seen that the few flows that are over the threshold in the LID scenario are much lower than the corresponding uncontrolled flows. This is partly because the low flow outflow from the orifice releases so much more runoff at rates below the threshold. This restores storage volume so that even large peaks can be reduced, as noted in Table 3 and Fig. 8.

Conclusions

Flows in bioretention-infiltration systems should be represented vertically in addition to the horizontal routing approaches typically used in conventional storm-water design. By judicious selection of orifice parameters and properties allocated to the suction node for surrounding soils, it is possible to realistically model the dynamics of the system using the power of a CS model applied to annual rainfall distribution. With this discrete routing approach, the benefits of urban retrofits can therefore be better

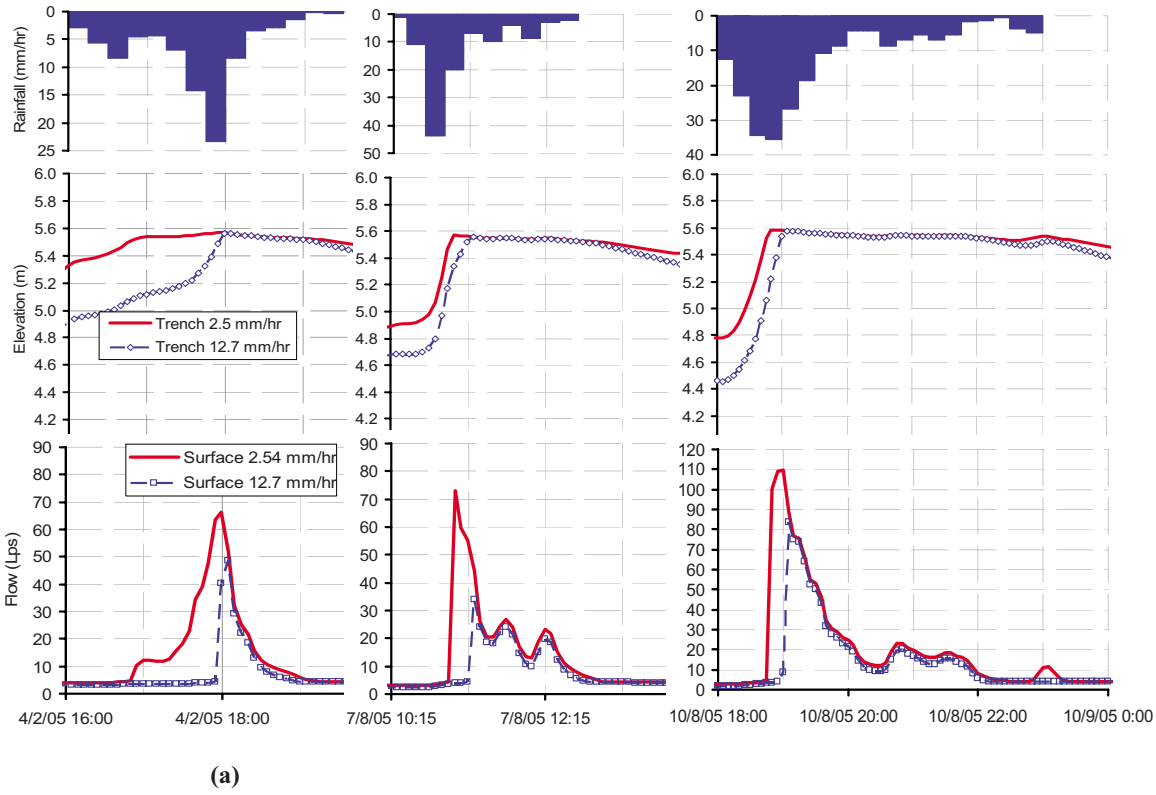

(a)

Fig. 8. Surface flow rates and node depths, 0.25 cm·h^{-1} and 1.27 cm·h^{-1} scenarios. (a) April 2, 2005; (b) July 8, 2005; and (c) October 8, 2005. Top row displays rainfall. Middle row displays trench elevations. Bottom row displays surface flow discharge. Note differing scales or rainfall and flow.

documented. The computational efficiency of this method of analysis can be applied to many discrete subcatchments to address specific outfall discharge criteria in a comprehensive manner, and under many scenarios.

The fact that the DS and CS models are inherently identical permits this approach to be used by both the CS and DS modeling communities to improve the design of urban retrofits. Systems designed to detain and/or infiltrate enough of the 5.08-cm event to reduce CSOs in the DS environment can give excellent annual performance under annual CS, both in terms of reducing CSOs, and in terms of retaining runoff. More sophisticated comparisons of CS and DS scenarios will be needed to better establish the shape and size of the controlling DS event(s) from both practical and cost-effective perspectives. Given stakeholder input, the appropriate DS distributions and corresponding discharge criteria can be formally established. Designers can then use the methods set forth in this paper to design effective SCM systems in the DS environment with which they are accustomed. A major benefit of this approach is that the HydroCAD DS interface is generally more responsive to user manipulation, so more alternatives can be easily evaluated. Furthermore, regulators with similar DS software can review the same assumptions to verify they meet the relevant criteria. In this way, the power of CS analysis can be leveraged to get better designs in the field using DS software.

Using this comprehensive approach at the street scale, the combined planter-trench system is capable of transforming the runoff response from an entirely impervious urban source areas into a runoff response more typically found in open space. If infiltration rates are even higher, the resulting runoff response could approach that of a forested condition. This is accomplished

Table 3. SWMM Routing Results, 2005 Design Year, Uncontrolled Runoff Compared to Planter Trench LID System, Infiltration Rates at 2.54 and 12.7 mm h^{-1}. Percentage reductions in flow and exceedances are shown in parentheses

Parameters	NoSCMs	LID planter-trench controlled inlet with and without suction routing			
K_{sat} (mm·h^{-1})	—	2.54	2.54	12.7	12.7
Suction head (cm)	—	0.0	15.0	0.0	6.4
Discharge (m^3)	1,175	680 (42%)	626 (47%)	277 (76%)	265 (77%)
Maximum total inflow (L−s^{-1})	252	112 (56%)	110 (56%)	85 (66%)	84 (66%)
Number of exceedances	233	6 (97%)	6 (97%)	4 (98%)	4 (98%)
Volume of exceedances (m^3)	635	72 (89%)	62 (90%)	35 (94%)	35 (95%)
Duration of exceedances (h)	199	20 (90%)	17 (91%)	11 (95%)	11 (95%)
Infiltrated volume (m^3)	—	504	553	905	912
Soil suction (m^3, % of infiltration)	—	—	121 (24%)	—	77 (15%)
Treated inflow (m^3, % of runoff)	—	520 (44%)	520 (44%)	526 (45%)	526 (45%)

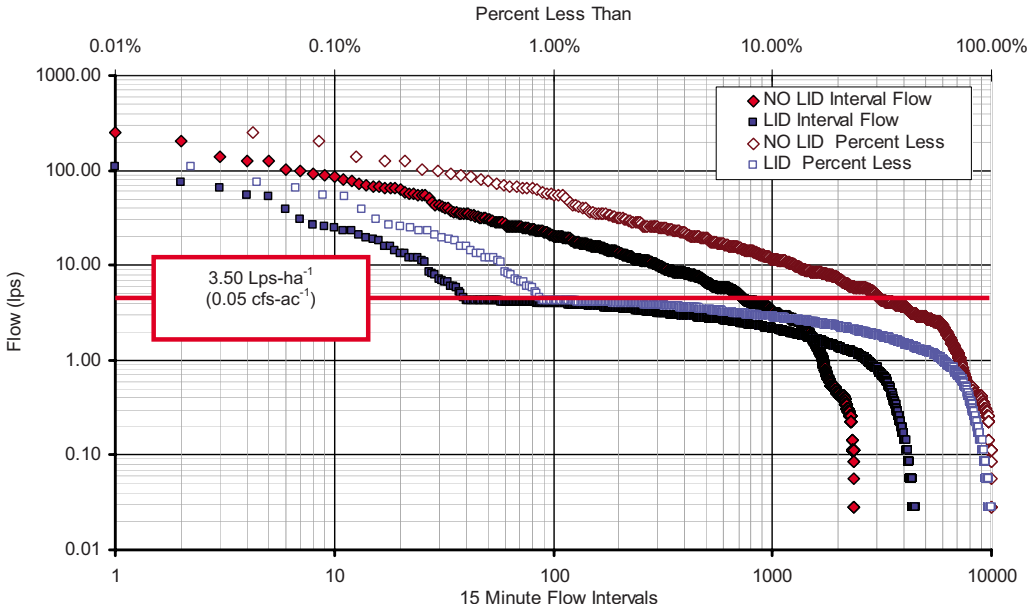

Fig. 9. Flow exceedance frequency and cumulative flow distribution: uncontrolled runoff compared to planter-trench LID system with K_{sat} of 2.54 mm·h^{-1} (0.10 in.·h^{-1})

with only 0.8% of the contributory source area used for the surface facility, in association with an underground trench system comprising an additional 3.4% of the source area. This result emphasizes the remarkable potential of LID design techniques to improve GI SCMs.

A promising enhancement of the trench system is to use structural soils to promote plant growth. Even though they provide for less storage, such systems would not only increase tree canopy cover and the beneficial effects of shade, it would also increase evapotranspiration, thus better restoring the water balance. These possibilities make integrated bioretention-infiltration systems a viable approach to contribute materially to Philadelphia's LTCP to reduce CSOs.

Acknowledgments

This work was done under a contract with Camp Dresser and McKee on behalf of the Philadelphia Water Department, Office of Watersheds. The writer wishes to express thanks to these organizations for the opportunity to undertake this analysis, and to thank CDM personnel for providing support in the design and modeling approach.

References

Bedient, P. B., and Huber, W. C. (1988). *Hydrology and floodplain analysis*, Addison-Wesley, Reading, Mass.

Blanco-Canqui, H., Gantzer, C. J., Anderson, S. H., and Alberts, E. E. (2004a). "Grass barriers for reduced concentrated flow induced soil and nutrient loss." *Soil Sci. Soc. Am. J.*, 68, 1963–1972.

Blanco-Canqui, H., Gantzer, C. J., Anderson, S. H., Alberts, E. E., and Thompson, A. L. (2004b). "Grass barrier and vegetative filter strip effectiveness in reducing runoff, sediment, nitrogen, and phosphorus loss." *Soil Sci. Soc. Am. J.*, 68, 1670–1678.

Culbertson, T. A., and Hutchinson, S. L. (2004). "Assessing bioretention cell function in a Midwest continental climate." *Proc., 2004 ASABE Annual Int. Meeting*, American Society of Agricultural and Biological Engineers, Ottawa.

Davis, A. P., Shokouhian, M., Sharma, H., and Minami, C. (2001). "Laboratory study of biological retention for urban storm-water management." *Water Environ. Res.*, 73(1), 5–14.

Hallam, L., and Carpenter, D. (2008). "An evaluation of planting soil mixtures on bioretention cell performance." *Proc., Low Impact Development 2008*, ASCE, Reston, Va.

Hatt, B. E., Fletcher, T. D., and Deletic, A. (2008). "Hydraulic and pollutant removal performance of fine media storm-water filtration systems." *Environ. Sci. Technol.*, 42(7), 2535–2541.

Hatt, B. E., Siriwardene, N., Deletic, A., and Fletcher, T. D. (2005). "Filter media for stormwater treatment and recycling: The influence of hydraulic properties of flow on pollutant removal." *Proc., 10th Int. Conf. on Urban Drainage*, Technical University of Denmark, Copenhagen.

Hunt, W. F., Smith, J. T., Shedlock, S. J., Hathaway, J. M., and Eubanks, P. R. (2008). "Pollutant loading and peak flow mitigation by a bioretention cell in urban Charlotte, N.C." *J. Environ. Eng.*, 134(5), 403–408.

James, W., et al. (2008). *User's guide to SWMM5*, Computational Hydraulics International, Guelph, Ont.

Le Coustumer, S., Fletcher, T. D., Deletic, A., and Barraud, S. (2007). "Hydraulic performance of biofilters for stormwater management: First lessons from both laboratory and field studies." *Water Sci. Technol.*, 56(10), 93–100.

Li, H., and Davis, A. P. (2008). "Urban particle capture in bioretention media. I: Laboratory and field studies." *J. Environ. Eng.*, 134(6), 419–432.

LimnoTech. (2009). "Case studies of hydrologic and hydraulic modeling efforts to support assessment of green infrastructure as a CSO mitigation measure." *Draft Rep. Prepared for U.S. EPA*.

Lucas, W. C., and Greenway, M. (2007). "A study of hydraulic dynamics in vegetated and non-vegetated bioretention mesocosms." *Proc., 7th Int. Conf. on HydroScience and Engineering (ICHE 2006)*, Drexel University, Philadelphia, ⟨http://idea.library.drexel.edu/bitstream/1860/1453/1/2007017108.pdf⟩ (April 5, 2010).

Nestingen, R. S., Asleson, B. C., Gulliver, J. S., Hozalski, M., and

Nieber, J. L. (2007). "Techniques to assess rain gardens as stormwater best management practices." *Proc., Stormwater and Urban Water Systems Modeling Conf.*, Computational Hydraulics International, Toronto.

Novák, V., Simunek, J., and van Genuchten, M. T. (2000). "Infiltration of water into soil with cracks." *J. Irrig. Drain. Eng.*, 126(1), 41–47.

Pitt, R. E. (1987). "Small storm flow and particulate washoff contributions to outfall discharges." Ph.D. thesis, Univ. of Wisconsin, Madison, Wis.

Rachman, A., Anderson, S. H., Gantzer, C. J., and Thompson, A. L. (2004). "Influence of stiff-stemmed grass hedge systems on infiltration." *Soil Sci. Soc. Am. J.*, 68, 2000–2006.

Ralston, M. R. (2004). "Fox hollow infiltration facility." *Proc., Putting the LID on Stormwater Management: 1st National Low Impact Development Conf.*, B. Rustia, ed., ASCE, Reston, Va.

Rose, C. W. (2004). *An introduction to the environmental physics of soil water and watersheds*, Cambridge University Press, Cambridge, U.K.

Saxton, K. E. (2005). "SPAW. Soil-plant-atmosphere-water field & pond hydrology operational manual." ⟨http://users.adelphia.net/~ksaxton/ftp%20files/SPAW%20Operational%20Manual-6.02.52.doc⟩ (July 8, 2008).

Saxton, K. E., and Rawls, W. J. (2006). "Soil water characteristic estimates by texture and organic matter for hydrologic solutions." *Soil Sci. Soc. Am. J.*, 70, 1569–1578.

Seobi, T., Anderson, S. H., Udawatta, R. P., and Gantzer, C. J. (2005). "Influence of grass and agroforestry buffer strips on soil hydraulic properties for an albaqualf." *Soil Sci. Soc. Am. J.*, 69, 893–901.

Sharma, S. K., Mohanty, B. P., and Zhu, J. (2006). "Including topography and vegetation attributes for developing pedotransfer functions." *Soil Sci. Soc. Am. J.*, 70, 1430–1440.